

VALIDATION EXPERIMENTS FOR MODELING SLOW COOK-OFF

Harold W. Sandusky and G. Paul Chambers
NAVSEA Indian Head Division
Indian Head, Maryland 20640-5035

William W. Erikson and Robert G. Schmitt
Sandia National Laboratories
Albuquerque, New Mexico 87185-0836

Slow cook-off experiments were conducted with measurements of temperature, pressure, and volume until the onset of ignition; time and position for onset of ignition; and reaction violence (case deformation and blast overpressure) following ignition. Confinement, gas sealing, and heating profile were varied in experiments on the RDX-based explosive PBXN-109 and on the HMX-based explosive PBXN-5. Pre- and post-ignition behavior for PBXN-109 was modeled for the experimental arrangement based on available characterization measurements for the heated explosive. While reasonable predictions of time for ignition are attained, the post-ignition wall expansion was over-predicted. More characterization of the enhanced burning rate for thermally degraded explosives is required to predict reaction violence.

INTRODUCTION

Cook-off is a complex process that is dependent on a variety of environmental factors including heating rate, confinement strength, free volume (ullage), and sealing of pyrolysis products. Since only a limited number of full-scale tests can be conducted, it would be advantageous to predict cook-off response for varying environments with computational models. Such models have evolved from simple expressions for explosion temperature, to global chemistry-based models,^{1,2} and finally to complex models³⁻⁶ including post-ignition burn dynamics capabilities. The simple models generally predict time-to-event for various energetic materials when boundary conditions are well known.

Moving beyond predictions of time-to-event to violence of reaction required theoretical model development and characterization of heated explosives. In the previous Detonation Symposium, models developed at Sandia National Laboratory, Albuquerque, NM (SNL/NM)^{3,7} and at Lawrence Livermore National Laboratory (LLNL)⁴ were evaluated against small-scale screening tests, such as the Variable Confinement Cook-off Test (VCCT),⁸ with some characterization^{9,10} of the properties for heated explosives. It was recognized that the models required further development, that more characterization of heated explosives was necessary for constitutive relations in these models, and that the models had to be validated.

Suitable metrics for comparing models and experiments include the rate of expansion of the energetic material, temperature at various locations within the energetic material and on the apparatus, strain in the confinement and pressure buildup within the confinement, evolution of gaseous decomposition products, time and position at which cook-off occurs, and the violence of that reaction. An experimental arrangement that is different than the usual closed pipe in most small-scale cook-off tests was developed to meet these requirements. It is described, along with data from it and model calculations.

This effort is part of a cooperative program that also includes LLNL and the Naval Air Warfare Center/China Lake (NAWC/CL). An instrumented closed pipe apparatus¹¹ at NAWC/CL has been modeled at both SNL/NM¹² and LLNL¹³. While several explosives have been studied, the main focus has been on the RDX-based explosive PBXN-109, whose properties when heated have recently been studied extensively.¹⁴⁻¹⁷

EXPERIMENTAL ARRANGEMENT

The apparatus¹⁸ in Figure 1 consists of a test cell mounted between flat springs in a load frame. Springs allow axial expansion of the test cell to reduce internal pressures from sample expansion and pyrolysis, so that seals are not breached without including ullage; and provide a means of continually measuring sample expansion. The 63.5 mm wide by 9.5 mm springs were clamped as shown in Figure 1, except in the last experiment where flexure was increased by removing the nuts on the same side as the test cell. There are spring stops to maintain the ends of the test cell sealed during cook-off.

Details of the test cell are shown in Figure 2. A cylindrical sample, 25.4 mm diameter by

63.5 mm long, is radially confined in a seamless mechanical tube of 1018 steel with variable thickness and axially confined with spring-loaded rams. The rams are sealed, the interface with the confinement tube by O-rings and the passages for internal thermocouples by epoxy. Tube thickness is varied by reducing the initial 31.7-mm outer diameter except at the ends. The tube is heated by resistance wire (0.25 mm nichrome wire with Teflon insulation) spiraled around it every 3.2 mm. A Phenolic spacer in each ram reduces heat losses to the springs. Temperature differences between the center of the sample and the rams were reduced from $\sim 15^{\circ}\text{C}$ in early experiments to 6°C in latter experiments by also wrapping resistance wire on the ends of the tube and on the exposed section of ram prior to the Phenolic spacer.

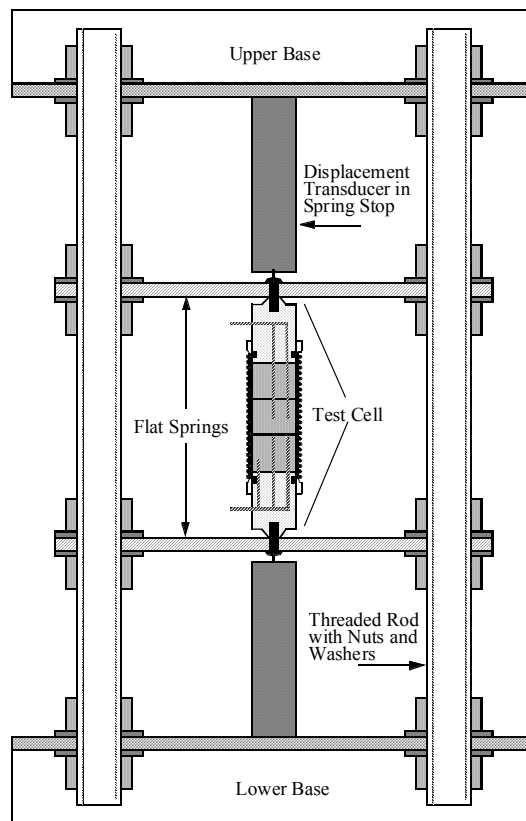


FIGURE 1. OVERALL APPARATUS

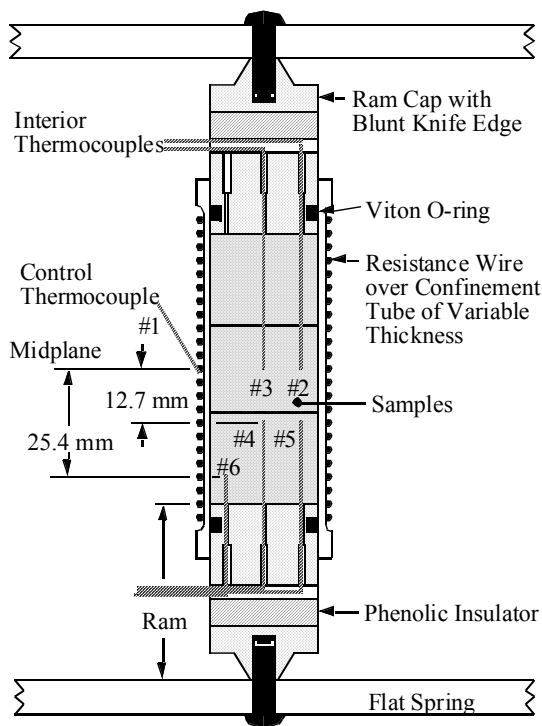


FIGURE 2. DETAILS OF TEST CELL

Temperatures were measured by copper-constantan thermocouples made from 0.25-mm diameter wires with Teflon insulation (Omega TT-T-30). These thermocouples were stiff enough to be inserted into 1-mm diameter holes drilled into the sample but small enough for minimal influence on sample temperature. External thermocouples often recorded lower temperatures than in the sample at the same axial plane because of the absence of any insulation on the tube exterior. That allowed an unobscured view of the tube but permitted heat loss from thermocouple junctions via cooler lead wires.

The mechanical measurements included circumferential strain at the midplane of the confinement tube and axial sample expansion. The preferable arrangement for tube strain had a high-temperature gage with minimal thermal output but limited strain capability (Micro-Measurements WK-06-250BG-350) for the heating cycle and a high-elongation gage (Micro-Measurements EP-08-125AC-350) for

cook-off. Axial sample expansion was equated to spring displacement, which was usually obtained with potentiometer-based displacement transducers. Spring displacement and confinement tube expansion were calibrated against interior pressure in the test cell before each experiment.

Dynamic diagnostics for cook-off included the high-elongation strain gage on the tube, a high-speed framing camera, and a transducer for blast overpressure at 0.6 m from the test cell. There is a clear field of view around the test cell for observing rapid expansion and fragmentation of the confinement tube. Photographs at ~100,000 frames/s were obtained with a Cordin 330 camera while back lighting the apparatus with an electronic flash triggered at the same time as the oscilloscopes for recording other dynamic diagnostics. Strain gages and a break wire around the midplane served as trigger probes.

Each sample consisted of three pieces, with a total mass of ~52 g. The PBXN-109 was from two sources, the same material used in the NAWC/CL tests¹⁰ and from NSWC-Yorktown. PBXN-5 pellets were pressed to that size from a locally available supply of molding powder.

EXPERIMENTAL RESULTS

Conditions and results from experiments intended to obtain a range of reaction violence are summarized in Table 1. Reaction violence includes amount of explosive consumed, number of fragments, and blast overpressure. These readily measured values are difficult for a model to compute; however, strain rate in the tube was both measured and calculated, and is a primary variable for fragmentation. Events listed in the last column follow definitions of tube fragmentation in the VCCT¹⁸ as a point of reference.

TABLE 1. SUMMARY OF EXPERIMENTAL CONDITIONS AND RESULTS

Shot CV-	Experimental Conditions				Results				
	Explosive	Heating Profile	Tube Wall Thickness	Ullage (%)	Cook-off T (°C)	Explosive Recovered	Frag. (No.)	P (kPa)	Event
1	PBXN-109 ¹	Ramp to 130°C, then 6°C/hr	0.050" 1.27 mm	~3.6	172	35%	4		Pressure Rupture
2	PBXN-109 ¹	Ramp to 150°C, then 3°C/hr	0.075" 1.90 mm	~3.6	170	6%	3		Pressure Rupture
3	PBXN-109 ²	Ramp to 150°C, then 3°C/hr	0.100" 2.54 mm	~1.0	165	Traces	6	86.9	Deflag.
4	PBXN-109 ²	Ramp to 130°C, then 3°C/hr	0.100" 2.54 mm	~1.0	162.5	4%	3	43.4	Pressure Rupture
5	PBXN-5 96.1 %TMD	Ramp to 140°C, then 3°C/hr	0.075" 1.90 mm	~1.0	195	Traces	8	135	Deflag.
6	PBXN-5 92.8 %TMD	Ramp to 140°C, then 3°C/hr	0.074" 1.89 mm	~1.0	202.4	Traces	18	83.4	Expl.

PBXN-109 with superscript 1 from NAWC/CL, with superscript 2 from NSWC-Yorktown

Frag. = Number of fragments

P = blast overpressure at 0.59 m from test cell

Event: pressure rupture, deflagration (Deflag.) or explosion (Expl.)

An experimental condition not listed in Table 1 is the combined spring deflection, which was usually ~1 mm/17 MPa. The corresponding ~2% increase in sample length prior to cook-off limited creation of porosity and reduction of density from thermal damage. The spring deflection was approximately doubled in the last experiment to allow more sample expansion.

PBXN-109 Experiments

The change in samples from NAWC/CL in Shots CV-1,2 to samples from NSWC-Yorktown in Shots CV-3,4 was for reducing an already small ullage so that thermal expansion could be observed during the initial heating to ~150°C. As the experiments progressed, the heating profile was altered to permit more time for thermal damage (combination of a lower temperature for the onset of slow heating and a lower heating rate), the confinement was increased, and the axial gradient in sample temperature was reduced, all in an effort to increase reaction violence. The only significant change in

reaction violence occurred in Shot CV-3, and that was from a loss of sealing.

The ~3.6% ullage in the first experiments accommodated thermal expansion without any pressure increase until ~150°C.¹⁸ As the heating continued, there was an exponential increase in pressure to 18.7 MPa and in sample length by 1.9% just prior to cook-off. When the ullage was reduced to ~1%, the pressure linearly increased from thermal expansion to 18.7 MPa at 150°C, and then exponentially increased to ~50 MPa just prior to cook-off in Shot CV-4. In Shot CV-3, the same trend occurred until thermocouple seals failed at 27.7 MPa.¹⁸

From the mechanical measurements, there is an ~150°C threshold for the onset of thermal damage at these rates of heating. In a separate study, PBXN-109 was recovered without damage after heating to 150°C in a similar timeframe.¹⁹ Reducing the 6°C/hr heating rate after Shot CV-1 to 3°C/hr allowed more time for thermal damage; however, with PBXN-109 remaining physically stable to ~150°C,

the lower starting temperature of 130°C for slow heating in Shot CV-4 would not have increased thermal damage beyond that in Shots CV-2,3. Thus, Shot CV-2 had a similar amount of recovered explosive and the same number of tube fragments, although for a somewhat thinner tube, as in Shot CV-4.

The first evidence of self-heating did not occur until 160 to 165°C. The temperature histories in Figure 3 for Shot CV-2 are for thermocouple locations specified in Figure 2. The two midplane locations had the same temperature until one hour before cook-off, at which time the center thermocouple began deviating. Cook-off was initiated in a small zone of thermal run-away not more than 10 mm in radius at a temperature of perhaps 200°C. Tabulated cook-off temperatures are those for the surrounding explosive and confinement, since the hot spot is seldom measured in tests. Samples from NAWC/CL had a cook-off temperature ~7°C higher than those from NSWC-Yorktown.

The more uniformly heated samples (6°C from midplane to rams) after Shot CV-1 would have increased thermal damage near the rams and facilitated reaction of explosive there. The cooler ends (~15°C), thinner tube wall, and faster heating rate in Shot CV-1 resulted in 35% of the explosive being recovered with some pieces as large as 10 mm, while 6% or less was recovered in millimeter size pieces in subsequent experiments.

High-elongation strain gages provided measurements at >5% strain, as shown in Figure 4. Without the tube in Shot CV-3 being pressurized just prior to cook-off, the strain rate during cook-off was higher than in Shot CV-4, corresponding to the increased number of fragments. Even so, there were only several small tube fragments in Shot SV-3 and a wall velocity of 42 m/s at 8% strain,

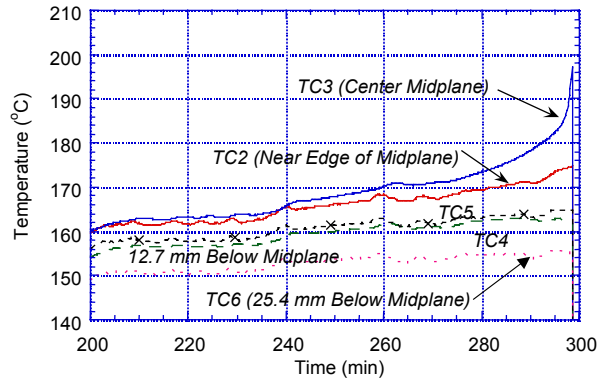


FIGURE 3. TEMPERATURES IN PBXN-109, SHOT CV-2

indicative of a burning reaction. The declining strain rate after 5% strain in Shot CV-4 was not real but rather a gage problem (probably a failing adhesive bond) according to camera measurements shown in the Modeling Section. The photographs also showed that the rams were still sealed when the tube began to rupture at the midplane upon attaining 30% strain.

Overpressure results from prompt reaction near the time of tube rupture. An overpressure in Shot CV-3 of twice that in Shot CV-4 correlates with the increased strain rate and twice the number of fragments, but not the small difference in explosive recovered. Much of the explosive burned after tube rupture without contributing to air blast.

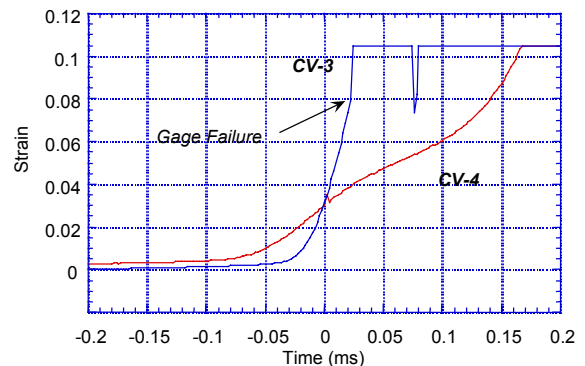


FIGURE 4. TUBE STRAIN DURING COOK-OFF IN SHOTS CV-3,4

PBXN-5 Experiments

The initial conditions of the two PBXN-5 experiments were the same except for the sample density and spring stiffness. The Shot CV-5 sample pellets were pressed to 96.1% of theoretical maximum density (TMD) and the arrangement had the same spring stiffness of previous experiments. Cook-off was a somewhat more vigorous deflagration than in PBXN-109 Shot CV-3 in terms of the number of fragments and the blast overpressure; however, the tube strain rate was similar.

The Shot CV-6 sample was pressed to a lower 92.8 %TMD and the spring stiffness was reduced to avoid eliminating the initial porosity in the sample as the pressure increased during heating, both in an effort to increase the cook-off violence. Pressures were ~24 MPa just prior to cook-off, versus ~40 MPa in Shot CV-5, corresponding to a sample expansion of 5.5%. PBXN-5 had less thermal expansion prior to cook-off as compared to PBXN-109, but an additional expansion from the HMX phase change.

The camera record in Shot CV-6 shows the onset of tube rupture at or somewhat above the interface between the top two sample pellets; unfortunately, no camera record was obtained in Shot CV-5. The interior temperature measurements in both shots (those for Shot CV-5 follow in the Modeling Section) showed slightly elevated temperature at 6.3 mm above the midplane. The onset of run away reaction away from the midplane, at least in Shot CV-6, may be responsible for a larger number of fragments but lower blast overpressure. With the apparatus oriented as in Figure 1, the upper half of the test cell has slightly elevated temperatures, which could shift the onset of run-away reaction; however, in Shot CV-6 the test cell was horizontally oriented to eliminate this variation. As shown in Figure 2, the thermocouples at the midplane

pass through the upper sample pellet, and these passages may be influencing the location for the onset of reaction. Since the thermocouples recorded little evidence of self-heating, its zone was probably small as PBXN-109. Based on the small size of some fragments recovered from Shot CV-6, the cook-off reaction is classed as an explosion.

MODELING

Pre-ignition Model

Thermophysical properties used for PBXN-109 are: density of 1.67 g/cc, specific heat varying from 0.24 to 0.36 cal/g-°C for temperatures from 0 to 200°C, thermal conductivity declining from 1.3 to 1.0×10^{-3} cal/cm-s-°C over the same temperature range, thermal expansion coefficient of 113 $\mu\text{m}/\text{m}-^\circ\text{C}$, and a bulk modulus from 1.8 to 6.1 GPa over a pressure range of 7.6 to 71 MPa.²⁰

The semi-global reaction schemes for PBXN-109 and PBXN-5 were based on the approach of McGuire and Tarver⁶. This approach has been relatively successful at matching event time in the one-dimensional time to explosion experiment (ODTX). Both schemes include three serial steps with four global chemical species: A, B, C, D. All three steps have Arrhenius kinetics (i.e., $k_i = A_i \exp[-E_{ai}/RT]$); steps 1 and 2 are first order in A and B respectively, and step 3 is second order in C. For PBXN-109, the heat of reaction in the McGuire and Tarver fit for RDX was adjusted to reflect the amount of RDX present, and then reaction parameters were fitted to ODTX data by using the XCHEM²¹ one-dimensional analysis code. Because of the nearly identical compositions for the HMX-based explosives PBXN-5 and LX-10, the original McGuire-Tarver⁶ chemistry model and properties for LX-10 were used for PBXN-5. The reaction

mechanism parameters for both explosives are listed in Table 2.

TABLE 2. GLOBAL REACTION MECHANISM STEPS FOR PBXN-109 AND PBXN-5

Explosive	Global Rxn Step	E_a (kcal/mole)	$\ln A$ (1/s)	Heat Release (cal/g)
PBXN-109	A → B	47.5	45.2	+64.9 (endo)
	B → C	45.0	40.0	-195 (exo)
	C → D	34.2	34.9	-779 (exo)
PBXN-5 (LX-10)	A → B	52.7	48.7	+100 (endo)
	B → C	44.1	37.5	-300 (exo)
	C → D	34.2	28.1	-1200 (exo)

The thermal analysis code Coyote²² was used to simulate heating and pyrolysis of the sample. The various components of the test cell in Figure 2 were represented an axisymmetric grid.¹² Ideally, heat losses and contact resistances were adjusted until external temperatures coincided with measurements, as illustrated in Figure 5 for PBXN-5 Shot CV-5. Calculated interior temperatures were then in reasonable agreement with measurements, as illustrated in Figure 6. Cook-off was calculated to originate from 4.8 mm above the midplane at 1123 min versus the measurement of 1164 min, with a calculated wall temperature of 191.9°C versus the measurement of 193.3°C. When measured external temperatures were lower than those in the apparatus, for the reasons previously discussed, external boundary conditions were adjusted until internal temperatures matched at the midplane during early times and were then assumed to continue with the same trend. With this approach, the prediction for cook-off in Shot CV-1 (Figure 7 of reference 12) was 36 minutes late and at a temperature 4°C higher, perhaps because the model over-predicted heat losses from the ends.

Post-ignition Model

A combustion model for energetic materials at various levels of damage²³ was used to describe the post-ignition behavior. A flame sheet is assumed with mass, momentum, and energy conserved across the discontinuity. The combustion process is initiated by

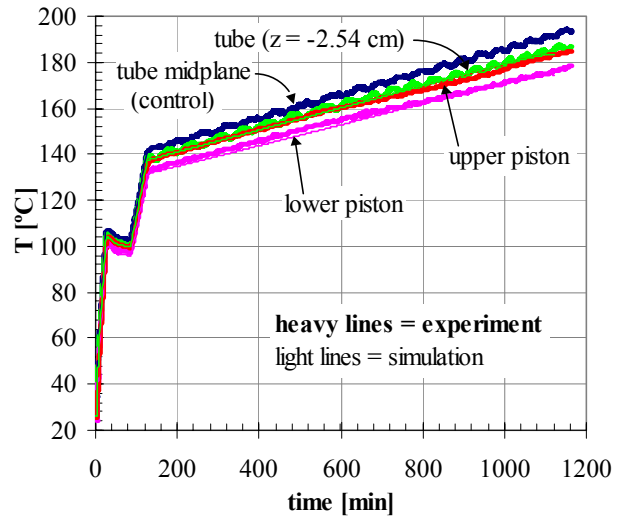


FIGURE 5. EXTERNAL TEMPERATURES IN SHOT CV-5, MODEL AND EXPERIMENT

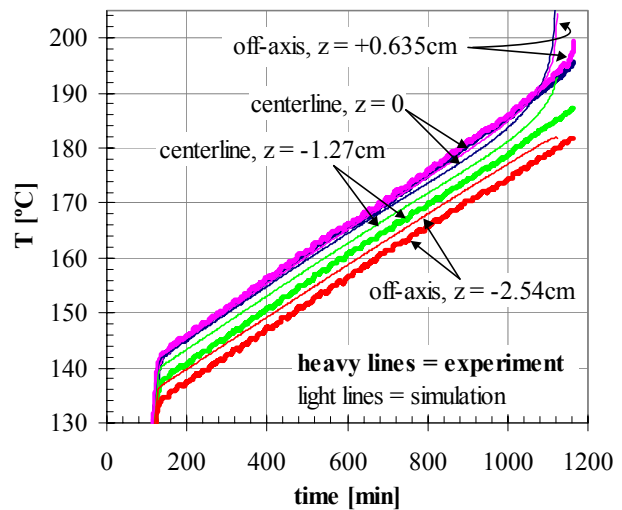


FIGURE 6. INTERNAL TEMPERATURES IN SHOT CV-5, MODEL AND EXPERIMENT

inserting a bubble of hot reaction products at elevated pressure into the matrix of unburned explosive. This model has been implemented into the arbitrary Lagrangian/Eulerian shock physics code, ALEGRA.²⁴

The sample and confinement were divided into a 2-dimensional axisymmetric grid.¹² Springs were modeled as a low modulus material near the outside end of the piston, which was fixed while the end of the piston within the tube could move from internal pressure. Both the unburned explosive and the steel confinement were treated as elastic-plastic materials with Mie-Gruneisen equations of state. The 1018 steel tube was modeled with a yield stress of 310 MPa and a hardening modulus of 758 MPa. Reaction products were treated as an ideal gas with a covolume non-ideal correction.

The burning model used a burning rate for pristine PBXN-109 in the form $r = AP^n$ (with $n = 1.4578$, $A = 4 \times 10^{-6}$, P in psi, r in in/s)¹⁴ that was then amplified. The 'A' parameter was increased by 20 to 30x until wall strains in the NAWC/CL tests were reproduced up to the maximum $\sim 1.5\%$ strain.¹² This burning rate enhancement was attributed to increased surface area from thermal damage.

In Figure 7, model calculations for tube expansion during cook-off of PBXN-109 are compared with measurements for Shot CV-4. A 30x enhancement gives a reasonable representation to about 1.5% strain; however, a 20x factor agrees better to about 4 to 5% strain, and 15x to about 15% strain. By extrapolation, $\sim 13x$ would match the remainder of the curve after 15% strain when a noticeable bend occurs in the data. It is not known whether this is caused by a change in the internal combustion dynamics, or by a plastic instability, or other phenomena occurring in the confinement material.

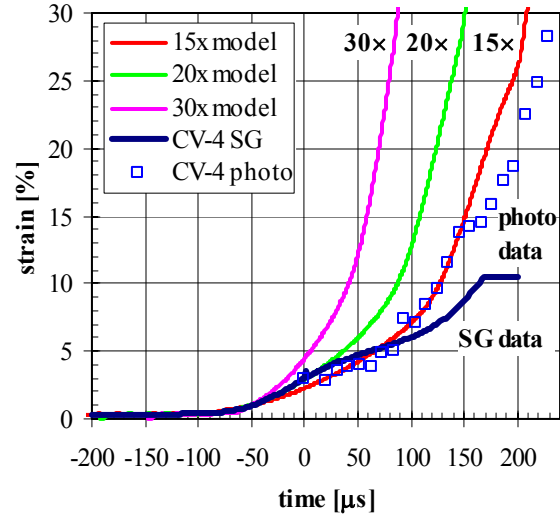


FIGURE 7. COMPARISON OF MODEL AND EXPERIMENT IN PBXN-109 SHOT CV-4

While enhancement factors can be adjusted to match results to particular data sets, we do not claim *predictive* capability for situations outside the original data. Moreover, as indicated in Figure 7, it appears that the surface area enhancement may not be constant throughout the combustion process (i.e. it is higher early in the burn, then subsequently decreases). If the 30x burning enhancement continued, strain rates of $\sim 8100 \text{ s}^{-1}$ would be reached at 30% strain compared to the more modest $\sim 3100 \text{ s}^{-1}$ observed in the data. A more fundamental model relating burning rates with damage level is clearly warranted.

SUMMARY AND CONCLUSIONS

Simultaneous mechanical and thermal measurements were made while slowly heating two explosives. In PBXN-109, there is significant pressure from thermal expansion when ullage is essentially eliminated, followed by an exponential increase in pressure from thermal damage and perhaps pyrolysis for three hours before cook-off. In PBXN-5, a comparable change in pressure

occurred from the phase change in HMX instead of thermal expansion, and the increase in pressure just prior to cook-off was much less. The zone of self-heating in PBXN-109 was in the center and relatively small, <10 mm radius. Self-heating in PBXN-5 occurred away from the center and was also small enough to have been mostly missed by the internal thermocouples. The shift in location was not from a change in experimental technique and may be related to gas seepage along internal thermocouples. Thermal models with global reactions predict time and temperature for cook-off when the temperature history is correctly calculated, which was challenging even for these controlled experiments.

While there were several measures of cook-off violence, tube strain was the result that could be most directly compared with calculations. Tube fragmentation, which is often a metric in testing, was related to strain rate but requires additional modeling for the confinement. Cook-off violence for PBXN-109 was insensitive to a range of parameters (factor of two increase in wall thickness, factor of two reductions in heating rate and axial thermal gradient) and classed as pressure bursts except for at most a deflagration when the pressure seal failed during heating. Initial expansion of the tube was modeled with burning rates 30x that for pristine explosive, indicating extensive thermal damage and elevated temperature at the site for the onset of reaction. That enhancement factor was less than 15x when the tube ruptured at 30% strain, by which time the reaction had propagated into cooler material with less thermal damage. In just two experiments there was a significant variation in cook-off violence for PBXN-5. Extensive fragmentation, which is classed as an explosion, occurred with several percent more porosity in the sample and twice the expansion permitted by the spring-loaded rams. Predictions of reaction violence are

presently possible only with calibration of enhanced burning in a similar environment.

ACKNOWLEDGEMENTS

This was a cooperative program with the Office of Naval Research funding experiments and the DoD/DOE Memorandum of Understanding supporting modeling under Technology Coordination Group III (Energetic Materials). Sandia is a multi-program laboratory operated by Sandia Corporation, a Lockheed Martin Company, for the United States Department of Energy under Contract DE-AC04-94AL85000.

REFERENCES

1. Bowden, F. P. and Yoffe, A. D., "Thermal Explosions," Chapter 3 of *Fast Reactions in Solids*, Butterworths Scientific Publication, London, 1958.
2. McGuire, R. R. and Tarver, C. M., "Chemical Decomposition Models for the Thermal Explosion of Confined HMX, TATB, RDX, and TNT Explosives," *7th Symposium (Int'l) on Detonation*, NSWC MP 82-334, 1981, pp. 56-64.
3. Baer, M. R., Hobbs, M. L., Gross, R. J., and Schmitt, R. G., "Cookoff of Energetic Materials," *11th Int'l Detonation Symposium*, Office of Naval Research, ONR 33300-5, 1998, pp. 852-861.
4. Nichols, A. L. III, Couch, R., McCallen, R. C., Otero, I., and Sharp, R., "Modeling Thermally Driven Energetic Response of High Explosives," *op. cit.*, pp. 862-871.
5. Matheson, E. R., Drumheller, D. S., and Baer, M. R., "A Coupled Damage and Reaction Model for Simulating Energetic Material Response to Impact Hazards," *APS Topical Conference on Shock Waves in Condensed Matter*, Snowbird UT, June, 1999.

6. Schmitt, R. G. et al., "Application of a Multiphase Mixture Theory with Coupled Damage and Reaction to the LANL Large-Scale Annular Cookoff Experiment," *JANNAF 19th Propulsion Systems Hazards Subcommittee (PSHS) Meeting*, CPIA Publ. 704, Vol. II, 2000, pp. 11-18.
7. Schmitt, R. G. et al., "Modeling Burn Rate Phenomena of Damaged Energetic Materials," *11th Int'l Detonation Symposium*, pp. 434-442.
8. Alexander, K., Gibson, K., and Baudler, B., *Development of the Variable Confinement Cookoff Test*, IHTR 1840, NAVSEA Indian Head Division, 1996.
9. Maienschein, J., and Chandler, J. B., "Burn Rates of Pristine and Degraded Explosives at Elevated Pressures and Temperatures," *11th Int'l Detonation Symposium*, pp. 872-879.
10. Renlund, A. M., et al., "Characterization of Thermally Degraded Energetic Materials," op. cit., pp. 127-134.
11. Atwood, A. I., Curran, P. O., Decker, M. W., and Boggs, T. L., "Experiments for Cookoff Model Evaluation," *JANNAF 19th PSHS Meeting*, Vol. I, Nov 2000, pp. 205-220.
12. Erikson, W. W. and R. G. Schmitt, "Pre- and Post-Ignition Modeling of Validation Cookoff Experiments," *JANNAF 20th PSHS Meeting*, April 2002, to be printed.
13. McClelland, M. A., Maienschein, J. L., Nichols, A. L., and Wardell, J. F., "ALE3D Model Predictions and Materials Characterization for the Cookoff Response of PBXN-109," op. cit.
14. Atwood, A. I. et al., "Experimental Input Parameters Required for Modeling the Response of PBXN-109 to Cookoff," *JANNAF 19th PSHS Meeting*, Vol. I, pp. 165-178.
15. Kaneshige, M. J., Renlund, A. M., and Schmitt, R. G., "Mechanical Response of Heated PBXN-109," op.cit., pp. 179-190.
16. McClelland, M. A. et al., "Cookoff Response of PBXN-109: Material Characterization and ALE3D Model," op.cit., pp. 191-204.
17. Maienschein, J. L. and Wardell, J. F., "Deflagration Behavior of PBXN-109 and Composition B at High Pressures and Temperatures," *JANNAF 20th PSHS Meeting*.
18. Sandusky, H. W. and Chambers, G. P., "Validation Experiments for Slow Cook-off," op.cit.
19. Kaneshige, M. J., SNL/NM, private communication, 2002.
20. Erikson, W. W., Schmitt, R. G., Atwood, A. I., and Curran, P. O., "Coupled Thermal-Chemical-Mechanical Modeling of Validation Cookoff Experiments," *JANNAF 19th PSHS Meeting*, Vol. II, pp. 53-65.
21. Gross, R. J., Baer, M. R., and Hobbs, M. L., "XCHEM-1D A Heat Transfer/Chemical Kinetics Computer Program for Multilayered Reactive Materials," SAND93-1603 UC-741, SNL/NM, 1993.
22. Gartling, D. K., Hogan, R. E., and Glass, M. W., "Coyote – A Finite Element Computer Program for Nonlinear Heat Conduction Problems," Version 3.0, Part 1 – Theoretical Background: SAND94-1173, Part 2 – User's Manual: SAND94-1179, SNL/NM, 1994.
23. Schmitt, R. G. and Baer, T. A., "Millisecond Burning of Confined Energetic Materials During Cookoff," *1997 JANNAF PSHS Meeting*, CPIA Publ. 657, Vol. I, 1997, pp. 61-71.
24. Summers, R. M. et al., "Recent Progress in ALEGRA Development and Application to Ballistic Impacts," SAND96-0045C, SNL/NM, 1996.